

Solubility of AlPO_4 and NaVO_3 in $\text{NaF}-\text{AlF}_3$ Melts

Marián Kucharík* and Roman Vasiljev

Institute of Inorganic Chemistry, Slovak Academy of Sciences, Dúbravská cesta 9, 845 36 Bratislava, Slovakia

The temperatures of primary crystallization of cryolite in systems $\text{NaF}-\text{AlF}_3-\text{AlPO}_4$ and $\text{NaF}-\text{AlF}_3-\text{NaVO}_3$ were determined by thermal analysis. The measurements were performed at cryolite ratios (CR) equal to 2.5 and 2 [$\text{CR} = n(\text{NaF})/n(\text{AlF}_3)$]. It is evident that AlPO_4 decreases the temperature of primary crystallization of cryolite more than NaVO_3 at both selected cryolite ratios.

Introduction

The industrial electrolyte of aluminum production (Hall–Héroult process) contains impurities, like iron, silicon, sulfur, phosphorus, vanadium, etc.¹ They are introduced to the electrolyte mainly through the raw materials (alumina and fluoride salts) and through anodes.² A small amount of vanadium or phosphorus impurities causes a significant decrease of current efficiency in the aluminum cell.³

Phosphorus can exist in different oxidation states, starting from -3 up to $+5$ and can form different compounds containing oxygen and fluorine. Therefore, the chemistry of phosphorus is very complex. A small amount of phosphorus in produced aluminum influences the quality of the metal. The phosphorus lowers the corrosion resistance and increases the brittleness of the metal.¹

Del Campo⁴ determined a phase diagram for the system $\text{Na}_3\text{AlF}_6-\text{Na}_4\text{P}_2\text{O}_7$ ($\text{CR} = 3$). Bratland et al.⁵ on the basis of del Campo's results considered reactions of the pyrophosphate anion ($\text{P}_2\text{O}_7^{2-}$) with the anions (AlF_6^{3-} , F^-) that form the PO_4^{3-} , PO_3F^{2-} , and PO_3^- anions. The AlF_6^{3-} and F^- anions are products of dissociation of molten cryolite.

The $\text{Na}_2\text{P}_4\text{O}_7$ compound was detected in solidified samples of the $\text{Na}_3\text{AlF}_6-\text{Na}_3\text{PO}_4$ molten system.⁶ When $\text{Al}(\text{PO}_3)_3$ was added to a cryolite melt, the formation of AlPO_4 and gaseous POF_3 was recorded by XRD and IR analysis.⁷

Thisted et al.⁸ measured a part of the phase diagram of the $\text{Na}_3\text{AlF}_6-\text{AlPO}_4$ system. The eutectic point was determined to be at 57.2 mol % AlPO_4 and (696 ± 1) °C. They suggested that in molten cryolite the orthophosphate anion PO_4^{3-} dissociates partly into metaphosphate PO_3^- and oxide ion O^{2-} .

Keppert et al.⁹ presented a new approach to the structure of the $\text{Na}_3\text{AlF}_6-\text{AlPO}_4$ molten system. They measured in situ high-temperature NMR spectra using a wide range of different nuclei involved in the $\text{Na}_3\text{AlF}_6-\text{AlPO}_4$ system: ^{19}F , ^{27}Al , ^{23}Na , ^{31}P , and ^{17}O . The PO_4 tetrahedron was found to be a stable structure in the cryolite-based melts. The chemical shift evolutions seemed to indicate the existence of the PO_4^{3-} and $(\text{AlF}_4-\text{O}-\text{PO}_3)^{4-}$ anions with an $\text{Al}-\text{O}-\text{P}$ bond. The ^{19}F NMR spectra excluded the presence of a $\text{P}-\text{F}$ bond (i.e., PO_3F^{2-} group) in $\text{Na}_3\text{AlF}_6-\text{AlPO}_4$ melts.

The solubility of vanadium pentoxide in pure cryolite and in cryolite–alumina melts was measured by Bratland et al.¹⁰ They used a visual method, and the determined solubility of V_2O_5 in

pure molten cryolite was 1.1 wt. % at 1030 °C. This result is in accordance with the older measurements of Rolin et al.¹¹ and Belyaev et al.¹² Bratland et al.¹⁰ also found that the solubility of V_2O_5 decreases linearly with increasing alumina content in molten cryolite.

Goodes and Algie¹³ investigated the distribution of vanadium impurities between the bath and aluminum and between the bath and gaseous phases, respectively. They detected residual vanadium in the bath, during the vanadium transfer across the bath/aluminum interface. Moreover, the content of vanadium in the bath was higher than reported by Bratland et al.¹⁰ The condensate from the fumes above the melt contained vanadium, particularly during the first (2 to 4) h of the runs, and then the volatilization seemed to cease. The reported differences can arise from the fact that different experimental conditions were considered.

Chrenková et al.¹⁴ studied the $\text{Na}_3\text{AlF}_6-\text{V}_2\text{O}_5$ system by thermal analysis. The authors concluded that the solubility of vanadium pentoxide in pure cryolite is higher than data reported in refs 10 to 12

Kucharík et al.¹⁵ measured the phase diagram of the $\text{Na}_3\text{AlF}_6-\text{NaVO}_3$ system. The system is a simple eutectic one. The eutectic point was estimated to be 97.5 mol % NaVO_3 and 617 °C. The XRD analysis of samples after thermal analysis revealed the presence of cryolite and NaVO_3 that supports the above assumption of a simple eutectic binary system. The thermodynamic calculation suggests that some reaction between molten cryolite and sodium metavanadate occurred.

Besides the lowering of the current efficiency, the vanadium impurities introduced into the bath have a negative influence on the quality of produced metal in a manner similar to phosphorus.¹

In this paper, we will present data on the primary crystallization in the $\text{NaF}-\text{AlF}_3-\text{AlPO}_4$ and $\text{NaF}-\text{AlF}_3-\text{NaVO}_3$ systems.

Experimental Section

For the preparation of samples, the following chemicals were used: natural hand-picked Na_3AlF_6 from Greenland (melting point: 1009 to 1011) °C), AlF_3 sublimated in a platinum crucible, NaF (Merck, 99.9 %), NaVO_3 (Aldrich, anhydrous, 99.9 %), AlPO_4 (Aldrich, 99.99 %), NaCl (Fluka, 99.9 %), and KCl (Fluka, 99.9 %). All chemicals were dried under vacuum at 150 °C for 5 h and handled in a glovebox under a dry nitrogen atmosphere (Messer, 99.99 %). The measurements of cooling

* Corresponding author. E-mail: uachkuch@savba.sk.

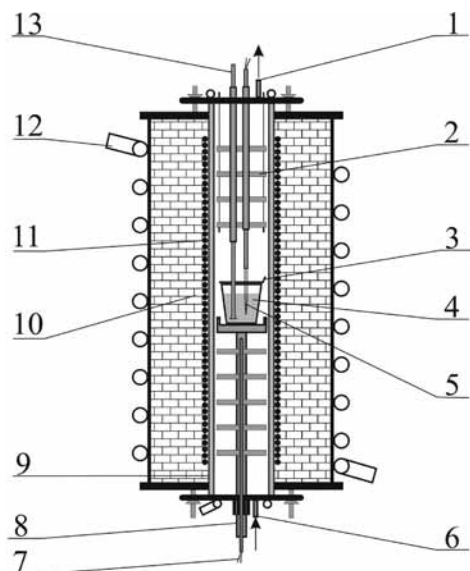


Figure 1. Cross section of the resistance furnace. 1, gas outlet; 2, corundum radiation shields; 3, platinum lid; 4, platinum crucible with melt; 5, Pt-PtRh10 measuring thermocouple; 6, gas inlet; 7, Pt-PtRh10 control thermocouple; 8, corundum sheath; 9, corundum tube (Alsint, 99.7 % Al_2O_3); 10, insulating material; 11, Kanthal heating element; 12, water cooling pipes; 13, platinum stirrer in corundum sheath.

Table 1. Compositions and Temperatures of Primary Crystallization ($t/^\circ\text{C}$) in the System $\text{NaF}-\text{AlF}_3-\text{AlPO}_4^a$

	$x(\text{NaF})$	$x(\text{AlF}_3)$	$x(\text{AlPO}_4)$	$t/^\circ\text{C}$
CR = 3	0.7500	0.2500	0	1011.0
	0.7481	0.2494	0.0025	1009.2
	0.7445	0.2482	0.0073	1005.2
	0.7403	0.2468	0.0129	1002.3
	0.7297	0.2432	0.0271	994.4
	0.7184	0.2395	0.0422	981.4
	0.7059	0.2353	0.0588	964.5
	0.6774	0.2258	0.0968	918.4
CR = 2.5	0.7143	0.2857	0	1003.0
	0.7107	0.2843	0.0050	995.8
	0.7072	0.2828	0.0100	990.2
	0.7000	0.2800	0.0200	979.0
	0.6929	0.2771	0.0300	967.6
	0.6786	0.2714	0.0500	945.7
	0.6607	0.2643	0.0750	905.0
	0.6429	0.2571	0.1000	862.6
CR = 2	0.6667	0.3333	0	954.0
	0.6634	0.3316	0.0050	940.0
	0.6600	0.3300	0.0100	941.1
	0.6534	0.3266	0.0200	925.0
	0.6467	0.3233	0.0300	890.0
	0.6334	0.3166	0.0500	878.8
	0.6167	0.3083	0.0750	827.0
	0.6000	0.3000	0.1000	783.3

^a Data for CR = 3 are from Thisted et al.⁸

curves were performed in a closed vertical resistance furnace with water-cooling and under an argon atmosphere (Messer, 99.996 %) (Figure 1). Mixtures of (10.000 ± 0.001) g with known composition were homogenized and transferred into a Pt crucible and placed in the furnace. The temperature was measured using a Pt-PtRh10 thermocouple calibrated with respect to the melting points of known compounds (NaCl, KCl, NaF, and Na_3AlF_6). The reproducibility of the measured temperatures was within ± 2 $^\circ\text{C}$. The cooling rate was 1.2 $^\circ\text{C}\cdot\text{min}^{-1}$. Each sample was kept for 12 h under an argon atmosphere in the furnace at 200 $^\circ\text{C}$ before the experiment. After the melting, the sample was homogenized by stirring with a platinum rod mounted on a corundum tube for 15 min.

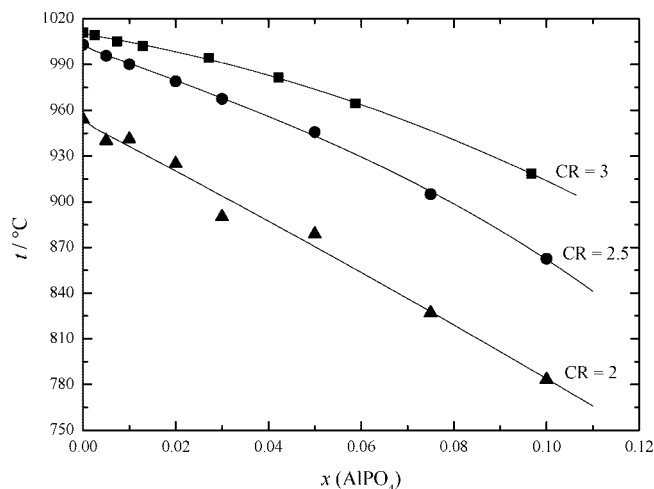


Figure 2. Temperatures of primary crystallization in the $\text{NaF}-\text{AlF}_3-\text{AlPO}_4$ system at different cryolite ratios, $\text{CR} = n(\text{NaF})/n(\text{AlF}_3)$. ■, CR = 3; ●, CR = 2.5; ▲, CR = 2. Data for CR = 3 are from Thisted et al.⁸

Table 2. Compositions and Temperatures of Primary Crystallization ($t/^\circ\text{C}$) in the System $\text{NaF}-\text{AlF}_3-\text{NaVO}_3^a$

	$x(\text{NaF})$	$x(\text{AlF}_3)$	$x(\text{NaVO}_3)$	$t/^\circ\text{C}$
CR = 3	0.75	0.25	0	1011
	0.7472	0.2491	0.0038	1007.1
	0.7423	0.2474	0.0103	1002.5
	0.7403	0.2468	0.0129	1001.3
	0.7297	0.2432	0.0271	996.6
	0.7183	0.2394	0.0423	991.5
	0.6923	0.2308	0.0769	982.2
	0.7143	0.2857	0.0000	1003.0
CR = 2.5	0.7107	0.2843	0.0050	998.0
	0.7072	0.2828	0.0100	996.2
	0.7000	0.2800	0.0200	992.4
	0.6929	0.2771	0.0300	987.9
	0.6786	0.2714	0.0500	982.0
	0.6607	0.2643	0.0750	974.9
	0.6667	0.3333	0.0000	954.8
	0.6634	0.3316	0.0050	951.5
CR = 2	0.6600	0.3300	0.0100	941.5
	0.6534	0.3266	0.0200	935.0
	0.6467	0.3233	0.0300	930.0
	0.6400	0.3200	0.0400	926.7
	0.6334	0.3166	0.0500	924.3

^a Data for CR = 3 are from Kucharík et al.¹⁵

Results and Discussion

The experimentally determined data for the $\text{NaF}-\text{AlF}_3-\text{AlPO}_4$ system are presented in Table 1 and for the $\text{NaF}-\text{AlF}_3-\text{NaVO}_3$ system are summarized in Table 2.

The graphical illustrations of primary crystallization temperatures versus composition are shown in Figure 2 ($\text{NaF}-\text{AlF}_3-\text{AlPO}_4$ system) and in Figure 3 ($\text{NaF}-\text{AlF}_3-\text{NaVO}_3$ system). It is evident that AlPO_4 decreases the temperature of primary crystallization more than NaVO_3 at identical compositions.

From results measured at CR = 2.5 and 2, it is not possible to conclude something about the structure of both molten systems, but it can be assumed that the obtained results (measurements and thermodynamic calculations) in the $\text{Na}_3\text{AlF}_6-\text{AlPO}_4$ system (CR = 3)⁸ or $\text{Na}_3\text{AlF}_6-\text{NaVO}_3$ system (CR = 3),¹⁵ respectively, will be approximately valid for cryolite ratios of 2.5 and 2.

Because high-temperature ^{19}F NMR measurements⁹ excluded the presence of the P-F bond in the $\text{Na}_3\text{AlF}_6-\text{AlPO}_4$ molten system, it can be assumed that the change of the cryolite ratios to lower values did not influence the product of AlPO_4

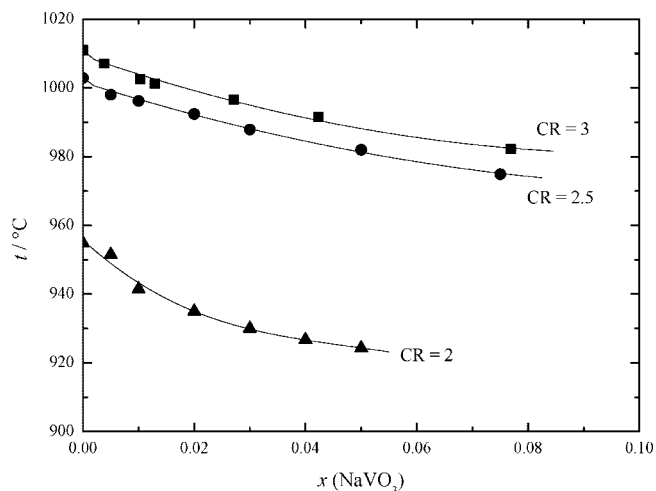


Figure 3. Temperatures of primary crystallization in the NaF–AlF₃–NaVO₃ system at different cryolite ratios, CR = $n(\text{NaF})/n(\text{AlF}_3)$. ■, CR = 3; ●, CR = 2.5; ▲, CR = 2. Data for CR = 3 are from Kucharík et al.¹⁵

dissolution in NaF–AlF₃ melts which should have been different phosphate anions.

In the case of the NaVO₃ in the NaF–AlF₃ molten system, an additional work, e.g., high-temperature NMR and Raman spectroscopy, should be performed as the next step for better understanding of dissolution process.

Generally, the measured data of primary crystallization temperatures are necessary for further physicochemical (density, viscosity, electrical conductivity, surface tension, etc.), electrochemical, and spectroscopic (HT NMR, HT Raman) measurements. Volume properties from density, electrochemical, and spectroscopic measurements are especially important for further study of the structure and also chemical and electrochemical reactions in these systems. Nowadays, cells in the aluminum industry work at cryolite ratios between 2 and 2.5, and therefore the measured data are interesting from a technological point of view.

Literature Cited

- (1) Grjotheim, K.; Krohn, C.; Malinovský, M.; Matiašovský, K.; Thonstad, J. *Aluminium Electrolysis, Fundamentals of the Hall-Héroult Process*, 2nd ed.; Aluminium-Verlag: Düsseldorf, Germany, 1982.
- (2) Thonstad, J.; Fellner, P.; Haarberg, G. M.; Híveš, J.; Kvande, H.; Sterten, Å. *Aluminium Electrolysis, Fundamentals of the Hall-Héroult Process*, 3rd ed.; Aluminium-Verlag: Düsseldorf, Germany, 2001.
- (3) Sterten, Å.; Solli, P. A.; Skybakmoen, E. Influence of electrolyte impurities on current efficiency in aluminium electrolysis cells. *J. Appl. Electrochem.* **1998**, *28*, 781–789.
- (4) Del Campo, J. J. La Electrolysis de la alumina en la criolita fundida, doctoral dissertation, Universidad de Oviedo, Escuela Tecnica Superior de Ingenieros de Minas Oviedo, Spain, 1984.
- (5) Bratland, D.; Kvande, H.; Bin, W. Q. Ionic species in cryolite-sodium pyrophosphate melts. *Acta Chem. Scand.* **1987**, *41A*, 377–380.
- (6) Daněk, V.; Chrenková, M.; Silný, A.; Haarberg, G.; Staš, M. Phosphorus in industrial aluminium cells. *Proc. Int. Terje Østvold Symp.*; Røros, Norway, 1998; pp 161–168.
- (7) Chrenková, M.; Daněk, V.; Silný, A. Reactions of phosphorus in molten cryolite. *X. Slovak-Norwegian Symposium on Aluminium Smelting Technology*; Stará Lesná, Slovakia, 1999; pp 89–92.
- (8) Thisted, E. W.; Haarberg, G. M.; Thonstad, J. Solubility of AlPO₄ in cryolite melts. *Thermochim. Acta* **2006**, *447*, 41–44.
- (9) Keppert, M.; Rakhmatullin, A.; Simko, F.; Deschamps, M.; Haarberg, G. M.; Bessada, C. Multinuclear magnetic resonance study of Na₃AlF₆–AlPO₄ molten and solidified mixture. *J. Magn. Reson.*, in press.
- (10) Bratland, D.; Campo, J. J.; Cho, K.; Grjotheim, K.; Thonstad, J. The solubility of vanadium pentoxide in molten cryolite-alumina and the aluminothermic reduction of vanadium pentoxide. *Light Metals* **1982**, *325*, 331.
- (11) Rolin, M.; Bernard, M. Solubilité des oxides dans la cryolite fondue. *Bull. Soc. Chim. France* **1963**, *1035*, 1038.
- (12) Belyaev A. I.; Rapoport M. B.; Firsanova L. A. *Elektrometallurgiya Alyuminiya*; Metallurgizdat: Moscow, 1953.
- (13) Goodes, C. G.; Algie, S. H. The partitioning of trace impurities between aluminium, cryolite and air - a laboratory study. *Light Metals* **1989**, *199*, 207.
- (14) Chrenková, M.; Silný, A.; Šimko, F. Reactions of Vanadium Oxide with Cryolite. *Chem. Pap.* **2005**, *59*, 85–88.
- (15) Kucharík, M.; Šimko, F.; Danielik, V.; Boča, M.; Vasiljev, R. Thermal analysis of the system Na₃AlF₆–NaVO₃. *Monatsh. Chem.* **2007**, *138*, 1211–1215.

Received for review March 3, 2008. Accepted May 4, 2008. The present work was financially supported by the Scientific Grant Agency of the Ministry of Education of the Slovak republic and the Slovak Academy of Sciences under the No. 2/7077/27.

JE800153N